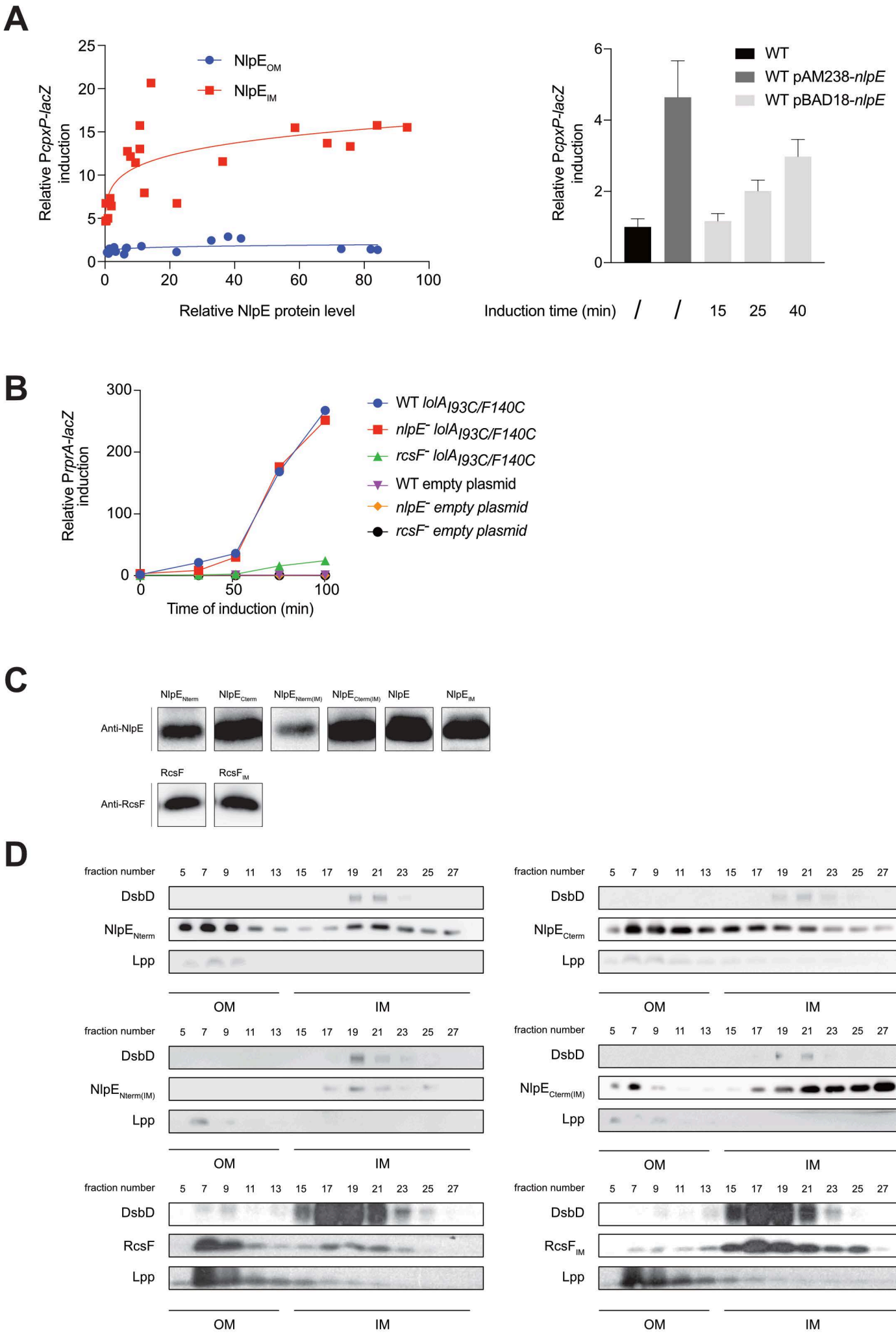
A
Relative PcpxP-lacZ induction
NlpE_OM
NlpE_IM
Relative NlpE protein level
WT
WT pAM238-nlpE
WT pBAD18-nlpE
Induction time (min) / / 15 25 40
B
Relative PprA-lacZ induction
WT lolA_I93C/F140C
nlpE- lolA_I93C/F140C
rcsF- lolA_I93C/F140C
WT empty plasmid
nlpE- empty plasmid
rcsF- empty plasmid
Time of induction (min)
C
NlpE_Nterm
NlpE_Cterm
NlpE_Nterm(IM)
NlpE_Cterm(IM)
NlpE
NlpE_IM
Anti-NlpE
RcsF
RcsF_IM
Anti-RcsF
D
fraction number
DsbD
NlpE_Nterm
NlpE_Cterm
NlpE_Nterm(IM)
NlpE_Cterm(IM)
RcsF
RcsF_IM
Lpp
OM
IM

Figure S1

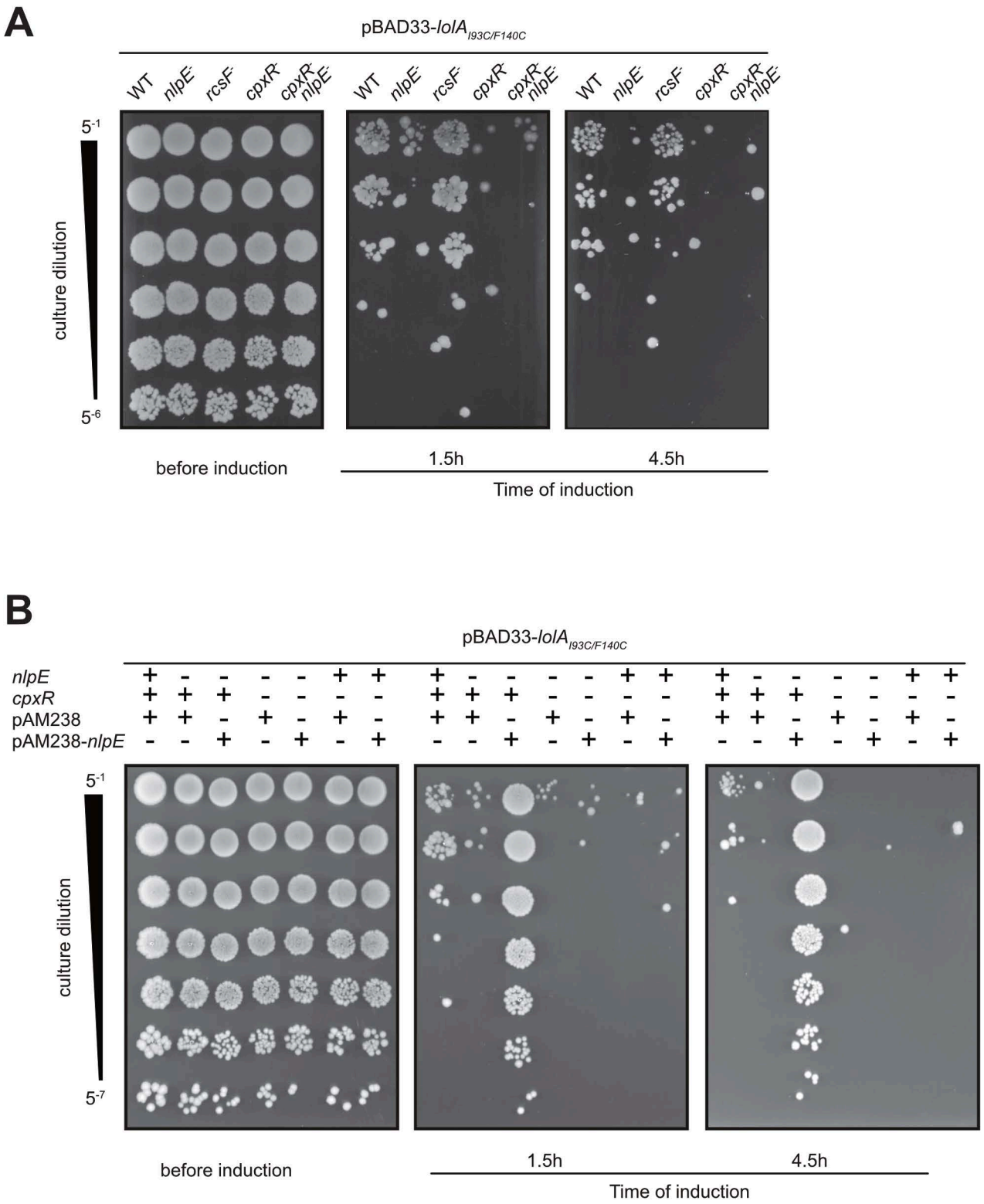
A
pBAD33-lolA I93C/F140C
WT
nlpE-
rcsF-
cpxR-
cpxR- nlpE-
5-1
5-6
culture dilution
before induction
1.5h
4.5h
Time of induction
B
pBAD33-lolA I93C/F140C
nlpE
cpxR
pAM238
pAM238-nlpE
5-1
5-7
culture dilution
before induction
1.5h
4.5h
Time of induction

Figure S2

SUPPLEMENTARY TABLES

Table S1. Strains and plasmids used in this study

Strain name	Genotype	Construction method	Source
PL442	MC4100 λRS88 [*cpxP′-lacZ*$^+$] *rcsF::kanR*	P1 transduction of *rcsF*::*kanR* from the Keio collection (2) into GL43	Pauline Leverrier
PL448	MC4100 λRS88 [*cpxP′-lacZ*$^+$] *dsbA::kanR*	P1 transduction of *dsbA*::*kanR* from the Keio collection (2) into GL43	Pauline Leverrier
GL16 = DH300	MG1655 D(argF-lac)U169 [*rprA142-lacZ*]		(1)
GL17 = PL339	MG1655 D(argF-lac)U169 [*rprA142-lacZ*] *rcsF::kanR*	P1 transduction of *rcsF*::*kanR* from the Keio collection (2) into GL43	Pauline Leverrier
GL18	MG1655 D(argF-lac)U169 [*rprA142-lacZ*] *nlpE::kanR*	P1 transduction of *nlpE*::*kanR* from the Keio collection (2) into GL16	This study
GL43 = PAD282	MC4100 λRS88 [*cpxP′-lacZ*$^+$]		(2)
GL44 = PL447	MC4100 λRS88 [cpxP′-lacZ+] *nlpE::kanR*	P1 transduction of *nlpE*::*kanR* from the Keio collection (2) into GL43	Pauline Leverrier
GL60	MC4100 λRS88 [*cpxP′-lacZ*$^+$] / pAM238-*nlpE*	Transformation of GL43 with pAM238-*nlpE*	This study
GL61	MC4100 λRS88 [*cpxP′-lacZ*$^+$] / pAM238	Transformation of GL43 with empty pAM238	This study
GL62	MC4100 λRS88 [*cpxP′-lacZ*$^+$] *nlpE::kanR* / pAM238-*nlpE*	Transformation of GL44 with empty pAM238-*nlpE*	(3)
GL63	MC4100 λRS88 [cpxP′-lacZ+] *nlpE::kanR* / pAM238	Transformation of GL44 with empty pAM238	This study
GL64 = PL461	MC4100 λRS88 [*cpxP′-lacZ*$^+$] Δ*dsbA*	Transformation of PL448 with pCP20 to flip out the FRT-*kanR*-FRT cassette	Pauline Leverrier

GL65 = PL464	MC4100 λRS88 [cpxP′-lacZ+] *nlpE::kan* Δ*dsbA*	P1 transduction of *nlpE*::*kanR* from the Keio collection (2) into PL461	Pauline Leverrier
GL73	MC4100 λRS88 [*cpxP′-lacZ*$^+$] *cpxR::kan*	P1 transduction of *cpxR*::*kanR* from the Keio collection (2) into GL43	(3)
GL97	MC4100 λRS88 [*cpxP′-lacZ*$^+$] pAM238-*nlpE(N22DN23D)*	Transformation of GL43 with pAM238-*nlpE(N22DN23D)*	This study
GL111	MC4100 λRS88 [cpxP′-lacZ+] *nlpE::kanR* / pAM238-*nlpE(Nt)*	Transformation of GL44 with pAM238-*nlpE(Nt)*	This study
GL165	MC4100 λRS88 [*cpxP′-lacZ*$^+$] / pAM238-nlpE*(NtN22DN23D)*	Transformation of GL43 with pAM238-*nlpE(NtN22DN23D)*	This study
GL146	MC4100 λRS88 [cpxP′-lacZ+] *nlpE::kanR* / pAM238-*nlpE(Ct)*	Transformation of GL44 with pAM238-*nlpE(Ct)*	This study
GL226	MC4100 λRS88 [cpxP′-lacZ+] *nlpE::kanR* / pBAD18-*nlpE*	Transformation of GL44 with pBAD18-*nlpE*	This study
GL228	MC4100 λRS88 [cpxP′-lacZ+] *nlpE::kanR* / pBAD18-*nlpE(N22DN23D)*	Transformation of GL44 with pBAD18-*nlpE(N22DN23D)*	This study
GL229	MC4100 λRS88 [*cpxP′-lacZ*$^+$] Δ*dsbA* *nlpE::nlpE(C51AC54A)*	λRed recombineering[a] at the *nlpE* locus in GL64 of *nlpE(C51AC54A)*, amplified with primers GL74 and GL75 with pET28-*nlpE(C51AC54A)* as a template	This study
GL245	MC4100 λRS88 [*cpxP′-lacZ*$^+$] / pAM238-*rcsF*	Transformation of GL43 with pAM238-*rcsF*	(3)
GL252	MC4100 λRS88 [*cpxP′-lacZ*$^+$] *nlpE::nlpE(C51AC54A)*	λRed recombineering[a] at the *nlpE* locus in GL43 of *nlpE(C51AC54A)*, amplified with primers GL74 and GL75 with pET28-	This study

		nlpE(C51AC54A) as a template	
GL285	MC4100 λRS88 [*cpxP′-lacZ*$^{+}$] / pAM238-*rcsF(CDD)*	Transformation of GL43 with pAM238-*rcsF(CDD)*	This study
GL372	MC4100 λRS88 [*cpxP′-lacZ*+] *nlpE::nlpE(C165AC231A)* Δ*dsbA*	λRed recombineering[a] at the *nlpE* locus in GL64 of *nlpE(C165AC231A)*, amplified with primers GL74 and GL75 with pAM238-*nlpE(C165AC231A)* as a template	This study
GL375	MC4100 λRS88 [cpxP′-lacZ+] *nlpE::nlpE(C165AC231A)*	λRed recombineering[a] at the *nlpE* locus in GL43 of *nlpE(C165AC231A)*, amplified with primers GL74 and GL75 with pAM238-*nlpE(C165AC231A)* as a template	This study
GL378	MC4100 λRS88 [cpxP′-lacZ+] Δ*cpxR*	Transformation of GL73 with pCP20 to flip out the FRT-*kanR*-FRT cassette	This study
GL442	MC4100 λRS88 [*cpxP′-lacZ*$^{+}$] / pBAD33	Transformation of GL43 with empty pBAD33	This study
AD34	MC4100 λRS88 [*cpxP′-lacZ*$^{+}$] / pBAD33-*lolA(I115CF162C)*	Transformation of GL43 with pBAD33-*lolA(I115CF162C)*	This study
AD35	MC4100 λRS88 [*cpxP′-lacZ*$^{+}$] *nlpE::kanR* / pBAD33-*lolA(I115CF162C)*	Transformation of GL44 with pBAD33-*lolA(I115CF162C)*	This study
AD50	MG1655 D(argF-lac)U169 [*rprA142-lacZ*] / pBAD33-*lolA(I115CF162C)*	Transformation of GL16 with pBAD33-*lolA(I115CF162C)*	This study
AD51	MG1655 D(argF-lac)U169 [*rprA142-lacZ*] *rcsF::kan* / pBAD33-*lolA(I115CF162C)*	Transformation of GL17 with pBAD33-*lolA(I115CF162C)*	This study

AD52	MG1655 D(argF-lac)U169 [*rprA142-lacZ*] *nlpE::kan* / pBAD33-*lolA(I115CF162C)*	Transformation of GL18 with pBAD33-*lolA(I115CF162C)*	This study
AD54	MC4100 λRS88 [*cpxP′-lacZ*$^{+}$] rcsF::kanR / pBAD33-*lolA(I115CF162C)*	Transformation of PL442 with pBAD33-*lolA(I115CF162C)*	This study
AD57	MC4100 λRS88 [cpxP′-lacZ+] *nlpE::kanR* / pBAD33	Transformation of GL44 with empty pBAD33	This study
AD63	MC4100 λRS88 [*cpxP′-lacZ*$^{+}$] *nlpE::kanR* / pBAD33-*lolA(I115CF162C)* / pAM238	Transformation of AD35 with empty pAM238	This study
AD64	MC4100 λRS88 [*cpxP′-lacZ*$^{+}$] *nlpE::kanR* / pBAD33-*lolA(I115CF162C)* / pAM238-*nlpE*	Transformation of AD35 with pAM238-*nlpE*	This study
AD112	MC4100 λRS88 [cpxP′-lacZ+] *nlpE::kanR* / pAM238-nlpE / pASKIBA-16-*Strep-cpxA(peri)*	Transformation of GL62 with pASKIBA-16-*Strep-cpxA(peri)*	This study
AD121	MC4100 λRS88 [cpxP′-lacZ+] *nlpE::kanR* / pAM238-nlpE / pASKIBA-16-*cpxA(peri)*	Transformation of GL62 with pASKIBA-16-*cpxA(peri)*	This study
AD155	MC4100 λRS88 [cpxP′-lacZ+] cpxR::kanR / pCDFDuet *α196 ω197*	Transformation of GL73 with pCDFDuet *α196 ω197*	This study
AD159	MC4100 λRS88 [cpxP′-lacZ+] cpxR::kanR / pCDFDuet *α196-nlpE ω197-cpxA*	Transformation of GL73 with pCDFDuet *α196-nlpE ω197-cpxA*	This study
AD160	MC4100 λRS88 [cpxP′-lacZ+] cpxR::kanR / pCDFDuet *α196 ω197-cpxA*	Transformation of GL73 with pCDFDuet *α196 ω197-cpxA*	This study
AD161	MC4100 λRS88 [cpxP′-lacZ+] cpxR::kanR / pCDFDuet *α196-nlpE ω197*	Transformation of GL73 with pCDFDuet *α196-nlpE ω197*	This study

AD162	MC4100 λRS88 [cpxP′-lacZ+] *nlpE::kanR* / pAM238-*nlpE* / pASKIBA-16	Transformation of GL62 with empty pASKIBA-16	This study
AD165	MC4100 λRS88 [cpxP′-lacZ+] *nlpE::kanR* / pAM238-*nlpE(Nt)* / pASKIBA-16-*Strep-cpxA(peri)*	Transformation of GL111 with pASKIBA-16-*Strep-cpxA(peri)*	This study
AD166	MC4100 λRS88 [cpxP′-lacZ+] *nlpE::kanR* / pAM238-*nlpE(Nt)* / pASKIBA-16-*cpxA(peri)*	Transformation of GL111 with pASKIBA-16-*cpxA(peri)*	This study
AD168	MC4100 λRS88 [cpxP′-lacZ+] *nlpE::kanR* / pAM238-*nlpE(Nt)* / pASKIBA-16	Transformation of GL111 with empty pASKIBA-16	This study
AD171	MC4100 λRS88 [*cpxP′-lacZ*$^{+}$] / pAM238-*nlpE(Nt)*	Transformation of GL43 with pAM238-*nlpE(Nt)*	This study
AD172	MC4100 λRS88 [*cpxP′-lacZ*$^{+}$] / pAM238-*nlpE(Ct)*	Transformation of GL43 with pAM238-*nlpE(Ct)*	This study
AD173	MC4100 λRS88 [cpxP′-lacZ+] *rcsF::kanR* / pBAD33	Transformation of PL442 with empty pBAD33	This study
AD174	MG1655 D(argF-lac)U169 [*rprA142-lacZ*] *nlpE::kanR*	Transformation of GL18 with empty pBAD33	This study
AD175	MG1655 D(argF-lac)U169 [*rprA142-lacZ*] *rcsF::kanR*	Transformation of GL17 with empty pBAD33	This study
AD178	MC4100 λRS88 [*cpxP′-lacZ*$^{+}$] Δ*cpxR* / pBAD33-*lolA(I115CF162C)*	Transformation of GL378 with pBAD33-*lolA(I115CF162C)*	This study
AD179	MC4100 λRS88 [*cpxP′-lacZ*$^{+}$] Δ*cpxR nlpE::kan* / pBAD33-*lolA(I115CF162C)*	Transformation of AD180 with pBAD33-*lolA(I115CF162C)*	This study
AD180	MC4100 λRS88 [*cpxP′-lacZ*$^{+}$] Δ*cpxR nlpE::kan*	P1 transduction of *nlpE*::*kanR* from the Keio collection (2) into GL378	This study
AD181	MC4100 λRS88 [*cpxP′-lacZ*$^{+}$] Δ*cpxR nlpE::kan* / pBAD33-	Transformation of AD179 with empty pAM238	This study

	lolA(I115CF162C) / pAM238		
AD182	MC4100 λRS88 [*cpxP′-lacZ*$^+$] Δ*cpxR nlpE::kan* / pBAD33-*lolA(I115CF162C)* / pAM238-*nlpE*	Transformation of AD179 with pAM238-*nlpE*	This study
AD183	MC4100 λRS88 [*cpxP′-lacZ*$^+$] Δ*cpxR* / pBAD33-*lolA(I115CF162C)* / pAM238	Transformation of AD178 with empty pAM238	This study
AD184	MC4100 λRS88 [*cpxP′-lacZ*$^+$] Δ*cpxR* / pBAD33-*lolA(I115CF162C)* / pAM238-*nlpE*	Transformation of AD178 with pAM238-*nlpE*	This study
AD185	MC4100 λRS88 [*cpxP′-lacZ*$^+$] / pBAD33-*lolA(I115CF162C)* / pAM238	Transformation of AD34 with empty pAM238	This study
AD187	MC4100 λRS88 [*cpxP′-lacZ*$^+$] / pAM238-*nlpE(CtN22DN23D)*	Transformation of GL43 with pAM238-*nlpE(CtN22DN23D)*	This study
AD191	MC4100 λRS88 [cpxP′-lacZ+] cpxR::kanR / pCDFDuet *α196-nlpE ω197-rcsC*	Transformation of GL73 with pCDFDuet *α196-nlpE ω197-rcsC*	This study
AD192	MC4100 λRS88 [cpxP′-lacZ+] cpxR::kanR / pCDFDuet *α196-rcsF ω197-cpxA*	Transformation of GL73 with pCDFDuet *α196-rcsF ω197-cpxA*	This study
AD200	MC4100 λRS88 [cpxP′-lacZ+] *nlpE::kanR* / pAM238 / pASKIBA-16-*cpxA(peri)*	Transformation of GL63 with pASKIBA-16-*cpxA(peri)*	This study
AD201	MC4100 λRS88 [cpxP′-lacZ+] *nlpE::kanR* / pAM238 / pASKIBA-16	Transformation of GL63 with empty pASKIBA-16	This study
JS471	MG1655 D(argF-lac)U169 [*rprA142-lacZ*] / pBAD33	Transformation of GL16 with empty pBAD33	Joanna Szewczyk
CH1990	MG1655 *yfaH::cat-sacB*		Diarmaid Hugues (Uppsala University)

Plasmid	Features, usage, resistance	Construction method	Source
pCP20	FLP^+, λ *c*I857$^+$, λ P_R Rep^{ts}, ampicillin, $Chlor^R$ (the vector is eliminated after transformation by overnight growth at 37°C)		(4)
pAM238	IPTG-regulated P_{lac} (in this study: constitutive expression without inducer), pSC101-based vector, $Spec^R$		(5)
pAM238-*nlpE*	Expression of wild-type *nlpE* from pAM238, $Spec^R$	Cloning of *nlpE* ORF and 28 upstream base pairs into pAM238 using KpnI and PstI	Joanna Szewczyk
pAM238-*nlpE(N22DN23D)*	Expression of $nlpE_{IM}$ from pAM238, $Spec^R$	Site-directed mutagenesis on pAM238-*nlpE* using primers GL48 and GL49	This study
pAM238-*nlpE(Nt)*	Expression of N-terminal domain of *nlpE* from pAM238, $Spec^R$	Cloning of *nlpE(Nt)* ORF, amplified from pAM238-*nlpE* with primers GL32 and GL35, into pAM238 using KpnI and HindIII	This study
pAM238-*nlpE(NtN22DN23D)*	Expression of N-terminal domain of $nlpE_{IM}$ from pAM238, $Spec^R$	Site-directed mutagenesis on pAM238-*nlpE(Nt)* using primers GL48 and GL49	This study
pAM238-*nlpE(Ct)*	Expression of C-terminal domain of *nlpE* from pAM238, $Spec^R$	Site-directed mutagenesis on pAM238-*nlpE* using primers GL65 and GL66	This study
pAM238-*nlpE(CtN22DN23D)*	Expression of C-terminal domain of $nlpE_{IM}$ from pAM238, $Spec^R$	Site-directed mutagenesis on pAM238-*nlpE(Ct)* using primers AD169 and AD170	This study
pAM238-*nlpE(C165AC231A)*	Template for λRed recombineering	Site-directed mutagenesis (2 rounds) on pAM238-*nlpE* using primers GL183-GL184, then GL185-GL186	This study
pET28-*nlpE(C51AC54A)*	Template for λRed recombineering		Pauline Leverrier

pBAD18	Arabinose-inducible P_{BAD}, pBR322-based, Amp^R		(6)
pBAD18-*nlpE*	Expression of *nlpE* from pBAD18, Amp^R	Cloning of *nlpE* ORF, amplified from GL15 with primers GL25 and GL32, into pBAD18 using KpnI and HindIII	This study
pBAD18-*nlpE(N22DN23D)*	Expression of $nlpE_{IM}$ from pBAD18, Amp^R	Restriction digestion of pAM238-*nlpE(N22DN23D)* with KpnI and HindIII, ligation into pBAD18	This study
pAM238-*rcsF*= pSC202	Expression of wild-type *rcsF* from pAM238, $Spec^R$		(7)
pAM238-*rcsF(CDD)* = pSC202(S17 D/M18D)	Expression of $rcsF_{IM}$ from pAM238, $Spec^R$		(7)
pBAD33	Arabinose-inducible P_{BAD}, pACYC184-based, Cm^R		(6)
pBAD33-*lolA*	Used as template for site-directed mutagenesis		Joanna Szewczyk
pBAD33-*lolA(I115CF162C)*		Site-directed mutagenesis (two rounds) of pBAD33-*lolA* with primers AD43-AD44, then AD45 and AD46	This study
pASKIBA-16	tet-inducible P_{BAD}, f1-based, contains Amp^R		IBA lifesciences
pASKIBA-16-*Strep-cpxA(peri)*	Expression of Strep-tagged periplasmic domain of *cpxA* from pASKIBA-16, Amp^R	Gibson assembly of PCR product with primers AD74 and AD77, pASKIBA-16 as template and primers AD75 and AD76 with GL43 as template	This study
pASKIBA-16-*cpxA(peri)*	Expression of un-tagged periplasmic domain of *cpxA* from pASKIBA-16, Amp^R	Gibson assembly of PCR product with primers AD78 and AD81, pASKIBA-16 as template and primers AD79 and AD80 with GL43 as template	This study

pCDFDuet *α196 ω197*	Co-expression of the *α196* and the *ω197* fragment of the TEM β-lactamase from the pCDFDuet plasmid		Gift from Shu Quan (East China University of Science and Technology)
pCDFDuet *α196-spy(dimer) ω197-Im7*	Used as template for cloning		Gift from Shu Quan (East China University of Science and Technology)
pCDFDuet *α196 ω197-Im7*	Used as template for cloning		Gift from Shu Quan (East China University of Science and Technology)
pCDFDuet *α196-spy(dimer) ω197*	Used as template for cloning		Gift from Shu Quan (East China University of Science and Technology)
pCDFDuet *α196-nlpE ω197-cpxA*	Co-expression of the *α196* and the *ω197* fragment of the TEM β-lactamase fused to *nlpE* and *cpxA* from the pCDFDuet plasmid	Gibson assembly of PCR products with primers AD130-AD131 and AD134-AD135 with pCDFDuet *α196-spy(dimer) ω197-Im7* as template and primers AD132-AD133 and AD136-AD137 with GL43 as template	This study
pCDFDuet *α196-nlpE ω197*	Co-expression of the *α196* (fused to *nlpE*) and the *ω197* fragment of the TEM β-lactamase from the pCDFDuet plasmid	Gibson assembly of PCR products with primers AD142-AD143 with pCDFDuet *α196-spy(dimer) ω197* as template and primers AD136-AD137 with GL43 as template	This study
pCDFDuet *α196 ω197-cpxA*	Co-expression of the *α196* and the *ω197* (fused to *cpxA*) fragment of the	Gibson assembly of PCR products with primers AD138-AD139 with pCDFDuet *α196 ω197-Im7*	This study

	TEM β-lactamase from the pCDFDuet plasmid	as template and primers AD132-AD133 with GL43 as template	
pCDFDuet *α196-nlpE ω197-rcsC*	Co-expression of the *α196* and the *ω197* fragment of the TEM β-lactamase fused to *nlpE* and *rcsC* from the pCDFDuet plasmid	Gibson assembly of PCR products with primers AD168-AD131 and AD171-AD135 with pCDFDuet *α196-spy(dimer) ω197-Im7* as template and primers AD158-AD159 and AD136-AD137 with GL43 as template	This study
pCDFDuet *α196-rcsF ω197-cpxA*	Co-expression of the *α196* and the *ω197* fragment of the TEM β-lactamase fused to *rcsF* and *cpxA* from the pCDFDuet plasmid	Gibson assembly of PCR products with primers AD164-AD165 with pCDFDuet *α196-nlpE ω197-cpxA* as template and primers AD162-AD163 with GL43 as template	This study

[a]2-step λRed recombineering (4): In a first step, *nlpE::cat-sacB* was amplified using primers GL72 and GL73 with CH1990 as template and incorporated by λRed recombineering in the indicated host strain. In a second step, λRed recombineering was used to replace *cat-sacB* by the indicated version of *nlpE,* a PCR product obtained with the indicated primers and template, leaving a scarless replacement of the native *nlpE.*

TABLE S2. Primers used in this study.

Primer	5'-3' sequence
GL25	AAAAAAAAGCTTTTACTGCCCCAAACTACTGCAAT
GL32	AAAAAAGGTACCAGCGGTCGGGAATAAAAAGAAGGAATGGATGGTG AAAAAAGCGATAGTGA
GL35	AAAAAAAAGCTTTTACGCTTCCAGCGTATAGTTGA
GL48	TCTTTACTCTGATGGGATGTGATGATCGGGCCGAAGTCGA
GL49	TCGACTTCGGCCCGATCATCACATCCCATCAGAGTAAAGA
GL65	CTCTGATGGGATGTAATAATGCACAATCCAGTTTACCTATG
GL66	CATAGGTAAACTGGATTGTGCATTATTACATCCCATCAGAG
GL72	GATGCGCGGCAAAGTGCGCAGCGGTCGGGAATAAAAAGAAGGAATG GATGAAAATGAGACGTTGATCGGCACG
GL73	ATATATCCTTCTGGCCTGTTTTGCGTTTGTTTCTGTCTCAAGACGGGTT AATCAAAGGGAAAACTGTCCA
GL74	GATGCGCGGCAAAGTGCGCAGCGGTCGGGAATAAAAAGA
GL75	ATATATCCTTCTGGCCTGTTTTGCGTTTGTTTCTGTCTCAAGACGGGTT ACTGCCCCAAACTACTGCAAT
GL183	TGCGGCGACCTTCACTGATGCCGCGACCGGAAAACGTTTC
GL184	GAAACGTTTTCCGGTCGCGGCATCAGTGAAGGTCGCCGCA
GL185	ATTTTACCCCAACCAGGATGCCAGTAGTTTGGGGCAGTAA
GL186	TTACTGCCCCAAACTACTGGCATCCTGGTTGGGGTAAAAT
AD43	CGCCGTTTATGCTGTGTGCCCGCAACCAGTCCAG
AD44	CTGGACTGGTTGCGGGCACACAGCATAAACGGCG
AD45	GATGGCACAATCCATCAGTGTAGCGCGGTGGAGCAGG
AD46	CCTGCTCCACCGCGCTACACTGATGGATTGTGCCATC
AD74	ATCTGGCGTGAATCGAGCTTACCACCACCACCACCAGATT
AD75	AATCTGGTGGTGGTGGTGGTAAGCTCGATTCACGCCAGAT
AD76	GGGACCGCGGTCTCGGCTTAGCGGTCAAACAGTAAGTTAA
AD77	ACTTACTGTTTGACCGCTAAGCCGAGACCGCGGTCCCGAA

AD78	ATCTGGCGTGAATCGAGCTTGGCCTGCGCTACGGTAGCGA
AD79	TCGCTACCGTAGCGCAGGCCAAGCTCGATTCACGCCAGAT
AD80	GGGACCGCGGTCTCGGCTTAGCGGTCAAACAGTAAGTTAA
AD81	ACTTACTGTTTGACCGCTAAGCCGAGACCGCGGTCCCGAA
AD130	ATCTGGCGTGAATCGAGCTTAGAACCACCACCACCAGAAC
AD131	GCAGTAGTTTGGGGCAGTAAGCAGATCTCAATTGGATATC
AD132	GTTCTGGTGGTGGTGGTTCTAAGCTCGATTCACGCCAGAT
AD133	TGGTGATGGCTGCTGCCTTAGCGGTCAAACAGTAAGTTAA
AD134	ACTTACTGTTTGACCGCTAAGGCAGCAGCCATCACCATCA
AD135	TCGACTTCGGCCCGATTATTAGAACCACCACCACCAGAAC
AD136	GTTCTGGTGGTGGTGGTTCTAATAATCGGGCCGAAGTCGA
AD137	GATATCCAATTGAGATCTGCTTACTGCCCCAAACTACTGC
AD138	TTAACTTACTGTTTGACCGCTAAGGCAGCAGCCATCACCA
AD139	ATCTGGCGTGAATCGAGCTTAGAACCACCACCACCAGAAC
AD142	ATTGCAGTAGTTTGGGGCAGTAAGCAGATCTCAATTGGAT
AD143	TCGACTTCGGCCCGATTATTAGAACCACCACCACCAGAAC
AD158	GTTCTGGTGGTGGTGGTTCTCATCAGCGAGAATCGGAAATTCG
AD159	TGGTGATGGCTGCTGCCTTAGCGAATGCGTTCCAGCACCT
AD162	TTCTGGTGGTGGTGGTTCTATGCGTGCTTTACCGATCTGT
AD163	GATATCCAATTGAGATCTGCTCATTTCGCCGTAATGTTAAGCGC
AD164	GCGCTTAACATTACGGCGAAATGAGCAGATCTCAATTGGATATC
AD165	ACAGATCGGTAAAGCACGCATAGAACCACCACCACCAGAA
AD168	CGATTCTCGCTGATGAGAACCACCACCACCAGAACCACCACCACCCC AAT
AD169	GATGATGCACAATCCAGTTTACCTATGACGCCGATGA
AD170	TGGATTGTGCATCATCACATCCCATCAGAGTAAAGAGG
AD171	ATTCGCTAAGGCAGCAGCCATCACCATCATCA

LEGEND FOR THE SUPPLEMENTARY INFORMATION

Figure S1. Sensitivity of the Cpx system towards NlpE localization and protein amounts, and levels of NlpE truncated variants. A. The Cpx system is sensitive to low levels of IM-localized NlpE. *Left:* Expression of $nlpE_{OM}$ (GL226) or $nlpE_{IM}$ (GL228) from the pBAD18 plasmid was induced for various amounts of time (ranging from 0 to 60 minutes of induction) with 0.2 % L-arabinose, then both β-galactosidase activity from P*cpxP-lacZ* and protein levels (via quantification of western blot analysis) were measured for each sample. Each point is a single sample measurement normalized to wild-type activity and protein level (GL43). Fit lines are non-linear log-log regression calculated with GraphPad Prism. *Right:* β-galactosidase activity from P*cpxP-lacZ* was measured in wild-type cells (GL43), in WT cells expressing *nlpE* from the pAM238 plasmid (GL60) or in WT cells expressing *nlpE* from the pBAD18 plasmid (GL226), in the same timeframe as the experiment on the left panel to compare constitutive *nlpE* overexpression from the pAM238 plasmid with *nlpE* expression conditions used in panel A. All values were normalized to the average activity obtained for GL43. Bars represent the average of normalized values from at least three independent clones. Error bars: standard deviations. **B.** Inducing the expression of $lolA_{I93C/F140C}$ leads to NlpE-independent and RcsF-dependent activation of the Rcs system. Wild-type (AD50), *rcsF::kanR* (AD51), *nlpE::kanR* (AD52) cells expressing $lolA_{I93C/F140C}$, as well as wild-type (JS471), *nlpE::kanR* cells (AD174) and *rcsF::kanR* cells (AD173) carrying the empty plasmid were induced with 0.2 % L-arabinose. β-galactosidase activity from P*rprA-lacZ* (a specific reporter of the Rcs system) was measured periodically. All values were normalized to the average activity obtained for JS471 after 150 min of growth. This graph is representative of at least 3 independent measurements. **C.** *Top:* Western blot using an

anti-NlpE antibody showing the levels of $NlpE_{Nterm}$, $NlpE_{Cterm}$, $NlpE_{Nterm(IM)}$, $NlpE_{Cterm(IM)}$, NlpE and $NlpE_{IM,}$ (strains GL165, AD171, AD172, AD187, GL60 and GL97 respectively). Shown is a representative image of 3 biological replicates. *Bottom:* Western blot using an anti-RcsF antibody showing that RcsF and $RcsF_{IM,}$ are detected at similar levels (strains GL165, AD171, AD172, AD187, GL60 and GL97 respectively). Shown is a representative image of 3 biological replicates. **D.** Cell lysates from cells expressing $NlpE_{Nterm}$, $NlpE_{Cterm}$, $NlpE_{Nterm(IM)}$, $NlpE_{Cterm(IM)}$, RcsF and $RcsF_{IM}$ (GL165, AD171, AD172, AD187, GL245 and GL285, respectively) were subjected to a two-step sucrose gradient to collect the membrane fraction and separate the OM from the IM. Final fractions were analyzed by Western blot using antibodies raised against NlpE or RcsF, Lpp (control for OM localization) and DsbD (IM control). Figure shows bands of NlpE or RcsF, Lpp and DsbD detected by Western blot, and the subcellular localizations are shown below the corresponding fractions for each strain. Data are from a representative experiment out of two repeats. Note that some of the overexpressed variants are not fully confined to one membrane; this is likely due to overexpression since this localization "leakiness" was less observed when NlpE was produced at native levels (3). Nevertheless, these data confirm that we could indeed modify the subcellular distribution of different constructs of NlpE and RcsF as expected from the lipoproteins sorting rules.

Figure S2. NlpE and the Cpx stress response provide a fitness advantage when lipoprotein sorting defects occur. A. Cpx confers a fitness advantage during lipoprotein sorting defects. $lolA_{I93C/F140C}$ was expressed from the pBAD33 plasmid in wild-type (AD34), *nlpE::kanR* (AD35), *rcsF::kanR* (AD54), Δ*cpxR* (AD178), Δ*cpxR nlpE::kanR* (AD179) cells before proceeding with serial dilution as indicated and spotting on LB agar to assess viability. This image is representative

of at least 3 independent replicates. **B.** The fitness defect due to *lolA*$_{I93C/F140C}$ can be complemented by overexpressing *nlpE*, but only if the Cpx can be activated (*i.e.* in the presence of *cpxR*). *lolA*$_{I93C/F140C}$ was expressed from the pBAD33 plasmid in the following strains (see Table S1 for more information): AD184, AD63, AD64, AD181, AD182, AD183, AD184, before proceeding with serial dilution as indicated and spotting on LB agar. This image is representative of at least 3 independent replicates.

Table S1. Strains and plasmids used in this study. Includes relevant genotypes and features, construction methods and sources.

Table S2. Primers used in this study. Includes primer names and sequences.

REFERENCES FOR THE SUPPLEMENTARY INFORMATION

1. **Majdalani N**, **Hernandez D**, **Gottesman S**. 2002. Regulation and mode of action of the second small RNA activator of RpoS translation, RprA. Mol Microbiol **46**:813–826.

2. **DiGiuseppe PA**, **Silhavy TJ**. 2003. Signal detection and target gene induction by the CpxRA two-component system. J Bacteriol **185**:2432–2440.

3. **Delhaye A**, **Collet JF**, **Laloux G**. 2016. Fine-Tuning of the Cpx Envelope Stress Response Is Required for Cell Wall Homeostasis in Escherichia coli. MBio **7**:e00047–16.

4. **Cherepanov PP**, **Wackernagel W**. 1995. Gene disruption in Escherichia coli: TcR and KmR cassettes with the option of Flp-catalyzed excision of the antibiotic-resistance determinant. Gene **158**:9–14.

5. **Gil D**, **Bouché JP**. 1991. ColE1-type vectors with fully repressible replication. Gene **105**:17–22.

6. **Guzman LM**, **Belin D**, **Carson MJ**, **Beckwith J**. 1995. Tight regulation, modulation, and high-level expression by vectors containing the arabinose PBAD promoter. J Bacteriol **177**:4121–4130.

7. **Cho S-H**, **Szewczyk J**, **Pesavento C**, **Zietek M**, **Banzhaf M**, **Roszczenko P**, **Asmar A**, **Laloux G**, **Hov A-K**, **Leverrier P**, **Van der Henst C**, **Vertommen D**, **Typas A**, **Collet JF**. 2014. Detecting Envelope Stress by Monitoring β-Barrel Assembly. Cell **159**:1652–1664.